Inorg. Chem. **2005**, *44*, 7194–7199

[1,2,5]Thiadiazolo[3,4-c][1,2,5]thiadiazolidyl: A Long-Lived Radical Anion and Its Stable Salts†

Alexander Yu. Makarov,[£] Irina G. Irtegova,[£] Nadezhda V. Vasilieva,[£] Irina Yu. Bagryanskaya,[£] Tobias Borrmann,[§] Yuri V. Gatilov,[£] Enno Lork,[‡] Ruediger Mews,*[,‡] Wolf-Dieter Stohrer,*[,§] and Andrey V. Zibarev*[,||]

Institute for Inorganic and Physical Chemistry, University of Bremen, 28334 Bremen, Germany

Received April 15, 2005

[1,2,5]Thiadiazolo[3,4-c][1,2,5]thiadiazole (**1**) is synthesized in 62% yield by fluoride ion-induced condensation of 3,4-difluoro-1,2,5-thiadiazole with $(Me_3SiN{=})_2S$. The reversible electrochemical reduction of **1** leads to the long-lived [1,2,5]thiadiazolo[3,4-c][1,2,5]thiadiazolidyl radical anion (**2**) and further to the dianion (**3**). The radical anion **2** is also obtained by the chemical reduction of the precursor **1** with *t*-BuOK in MeCN. The radical anion **2** is characterized by ESR spectroscopy in solution and in the crystalline state. The stable salts [K(18-crown-6)][**2**] and [K(18-crown-6)][**2**]·MeCN (**8** and **9**, respectively) are isolated from the spontaneous decomposition of the [K(18-crown-6)][PhXNSN] (**6**, X = S; **7**, X = Se) salts in MeCN solution followed by XRD characterization. The radical anion **2** acts as a bridging ligand in **8** and as chelating ligand in **9**. The structural changes observed by XRD in going from **1** to **2** are explained by means of DFT/(U)B3LYP/6-311+G* calculations.

Introduction

The design, synthesis, and investigation of new molecular materials, especially of conducting, superconducting, and magnetic materials, belong to the topical fields of current scientific and technological progress. Over the past two decades, there has been considerable interest in the syntheses, molecular and electronic structures, and physical properties of heterocyclic thiazyl radicals, neutral and charged, recognized as promising building blocks for new molecular magnets and/or molecular conductors.[1] In the solid state, some thiazyl radicals demonstrate spin-state crossover accompanied by magnetic hysteresis.[2] The bistability arises from the coexistence over a temperature range of two solid state phases, one based on paramagnetic radicals, the other on their weakly bonded diamagnetic dimers. It is believed that corresponding magnetically bistable materials can find applications in molecular spintronic devices, i.e., in magneto-thermal and magneto-optical switching and information storage devices.[2,3]

Numerous neutral and positively charged heterocyclic thiazyl radicals (radical cations) have carefully been explored, while rather rare negatively charged systems (radical anions) have been less studied.[1,2,4−7] In this context, new precursors to heterocyclic thiazyl radical anions are especially desirable.

† This work was jointly supported by the DFG, Germany (Grant Nos. 436 RUS 113/486/0-2 R, 436 RUS 17/84/04), and the RFBR, Russia (Grant No. 02-03-04001).

* To whom correspondence should be addressed. Fax: (+ 49) 421-218-4267 (R.M.); (+ 49) 421-218-3720 (W.-D.S.); (+ 7) 383-330-9752 (A.V.Z.). E-mail: mews@chemie.uni-bremen.de (R.M.); stohrer@chemie.uni-bremen.de (W.-D.S.); zibarev@nioch.nsc.ru (A.V.Z.).

‡ Institute for Inorganic and Physical Chemistry, University of Bremen, 28334 Bremen Germany.

§ Institute for Organic Chemistry, University of Bremen, 28334 Bremen, Germany.

£ Institute of Organic Chemistry, Russian Academy of Sciences, 630090 Novosibirsk, Russia.

|| Department of Physics, Novosibirsk State University, 630090 Novosibirsk, Russia.

(1) (a) Rawson, J. M.; Palacio, F. *Struct. Bonding* **2001**, *100*, 93−128. (b) Boere, R. T.; Roemmele, T. L. *Coord. Chem. Rev.* **2000**, *210*, 369−445. (c) Rawson, J. M.; McManus, G. D. *Coord. Chem. Rev.* **1999**, *189*, 135−168. (d) Rawson, J. M.; Banister A. J.; Lavender I. *Adv. Heterocyclic Chem.* **1995**, *62*, 137−247. (e) Cordes, A. W.; Haddon, R. C.; Oakley, R. T. *Adv. Mater.* **1994**, *6*, 798−802. (f) Parsons, S.; Passmore, J. *Acc. Chem. Res.* **1994**, *27*, 101−108. (g) Oakley, R. T. *Prog. Inorg. Chem.* **1988**, *36*, 299−391.

(2) (a) Fujita, W.; Agawa, K. *Synth. Met.* **2003**, *137*, 1263−1265. (b) Fujita, W.; Agawa K. *Science* **1999**, *286*, 261−262.

(3) Itkis, M. E.; Chi, X.; Cordes, A. W.; Haddon, R. C. *Science* **2002**, *296*, 1443−1445.

(4) Fujita, W.; Agawa, K.; Takahashi, M.; Takeda, M.; Yamazaki, T. *Chem. Phys. Lett.* **2002**, *362*, 97−102. (b) Fujita, W.; Agawa, K. *Chem. Phys. Lett.* **2002**, *357*, 385−388.

(5) (a) Kaszynski, P. *J. Phys. Chem. A* **2001**, *105*, 7626−7633. (b) Kaszynski, P. *J. Phys. Chem. A* **2001**, *105*, 7615−7625.

(6) (a) Cameron, T. C.; Lemaire, M. T.; Passmore, J.; Rawson, J. M.; Shuvaev, K. V.; Thompson L. K. *Inorg. Chem.* **2005**, *44*, 2576−2578. (b) AnTorrena, G.; Brownridge, S.; Cameron, S. T.; Palacio, F.; Parsons, S.; Passmore, J.; Thompson, L. K.; Zarlaida, F. *Can. J. Chem.* **2002**, *80*, 1568−1583.

10.1021/ic050583j CCC: $30.25
Published on Web 08/31/2005

Table 1. Crystal Data and Structure Refinement for **1**, **6**, **7**, **8**, and **9**

compounds	**1**	**6**	**7**	**8**	**9**
empirical formula	$C_2N_4S_2$	$C_{18}H_{29}KN_2O_6S_2$	$C_{18}H_{29}KN_2O_6SSe$	$C_{14}H_{24}KN_4O_6S_2$	$C_{16}H_{27}KN_5O_6S_2$
fw	144.18	472.66	519.56	447.59	488.65
temp (K)	173(2)	173(2)	173(2)	193(2)	193(2)
wavelength (pm)	71.073	71.073	71.073	71.073	71.073
cryst syst	monoclinic	orthorhombic	orthorhombic	triclinic	monoclinic
space group	$P2_1/c$	$P2_12_12_1$	$P2_12_12_1$	$P\bar{1}$	$P2_1/m$
a (pm)	377.70(10)	924.40(10)	817.0(3)	824.99(11)	812.56(3)
b (pm)	1048.1(2)	1563.7(2)	1665.1(13)	855.19(13)	1493.43(4)
c (pm)	631.8(2)	1609.4(2)	1739.0(6)	911.63(11)	937.74(4)
α (°)	−	−	−	71.096(4)	−
β (°)	105.76(2)	−	−	63.441(5)	100.023(1)
γ (°)	−	−	−	64.862(4)	−
V (nm^3)	0.24071(11)	2.3264(5)	2.366(2)	0.51363(12)	1.12058(7)
Z	2	4	4	1	2
ρ_{calcd} (mg m^{-3})	1.989	1.350	1.459	1.447	1.448
abs coeff (mm^{-1})	0.968	0.442	1.885	0.499	0.465
crystal size (mm^3)	0.90 × 0.70 × 0.15	0.60 × 0.50 × 0.40	0.70 × 0.20 × 0.20	0.08 × 0.25 × 0.30	0.30 × 0.35 × 0.61
reflns collected	2157	3389	3109	5567	8046
independent reflns	549 (R_{int} = 0.0512)	3054 (R_{int} = 0.0312)	2795 (R_{int} = 0.0644)	2803 (R_{int} = 0.0257)	3101 (R_{int} = 0.0169)
final R indices [$I > 2\sigma(I)$][a]	R_1=0.0479	R_1 = 0.0677	R_1 = 0.0589	R_1 = 0.0481	R_1 = 0.0498
R indices (all data)	wR_2=0.1310	wR_2 = 0.1839	wR_2 = 0.1460	wR_2 = 0.1586	wR_2 = 0.1607

[a] $R1 = \sum||F_o| - |F_c||/\sum|F_o|$; $wR2 = \{\sum[w(F_o^2 - F_c^2)^2]/\sum[w(F_o^2)^2]\}^{1/2}$.

The chemistry of [1,2,5]thiadiazolo[3,4-c][1,2,5]thiadiazole (**1**), the 10π-electron hetero-analogue of naphthalene, has so far received little attention.[8] It has however been shown by ESR spectroscopy that the reduction of **1** with Na in THF leads to the [1,2,5]thiadiazolo[3,4-c][1,2,5]thiadiazolidyl (**2**) radical anion.[8c]

In this paper, we describe the electrochemical generation of **2** and its isolation in the form of stable salts. This radical anion might be of interest to materials science as a building block for molecular ion-based conductors and/or magnets.[1,2,9]

Experimental Section

The ^1H, ^{13}C, ^{14}N, ^{15}N, ^{29}Si, and ^{77}Se NMR spectra were measured with a Bruker DRX-500 spectrometer at frequencies of 500.13, 125.76, 36.13, 50.68, 99.33, and 95.38 MHz, respectively, with TMS, NH_3(l), and Me_2Se as standards. High-resolution mass spectra were recorded with a Finnigan MAT MS 8200 mass spectrometer. UV−vis spectra were taken on a Hewlett-Packard 8453 instrument.

CV measurements on **1** were performed at 25 °C in an argon atmosphere in absolute MeCN at a stationary platinum electrode with 0.1 M Et_4NClO_4 as supporting electrolyte, with scan rates of 0.05−50 V s^{-1}. Comparative measurements on **1** and naphthalene were carried out under the same conditions, with a mixture of 0.1 M Bu_4NBF_4 and 0.033 M Et_4NClO_4 as supporting electrolyte. Peak potentials are quoted with reference to a saturated calomel electrode.

ESR spectra were recorded on a Bruker ESP-300 spectrometer (MW power 265 mW, modulation frequency 100 kHz, modulation amplitude 0.005 mT), under anaerobic conditions. The spectral integrations and simulations were performed with the Winsim 32 program (accuracy of a(N) is ±0.001 mT). The g-factor of **2** was measured using an MnO standard with an accuracy of ±0.0002.

The XRD data (Table 1) for **1**, **6**, and **7** were collected on a Siemens P4 diffractometer using Mo Kα (λ = 71.073 pm) radiation with a graphite monochromator and for **8** and **9** on a Bruker-Nonius X8Apex CCD diffractometer with Mo Kα radiation using ϕ scans of narrow (0.5°) frames. The structures were solved by direct methods and refined by full-matrix least-squares method against all F^2 in anisotropic approximation using the SHELX-97 programs set.[10] Absorption corrections were applied empirically using DIFABS (**7**) and SADABS (**8**, **9**) programs.[10,11] Tables listing detailed crystallographic data, atomic positional parameters, and bond lengths and angles are available as CCDC-263633 (**1**), CCDC-276847 (**6**), CCDC-276848 (**7**), CCDC-263635 (**8**), and CCDC 263634 (**9**) at the Cambridge Crystallographic Data Centre.

Quantum chemical calculations were performed with the GAUSSIAN 98 set of programs.[12]

Synthesis of 1. Under argon, a solution of 3.66 g (0.03 mol) of 3,4-difluoro-1,2,5-thiadiazole[13] and 6.18 g (0.03 mol) of $(Me_3SiN{=})_2S$[14b] in 10 mL of absolute MeCN was added dropwise during 1 h to a refluxed and stirred suspension of 9.12 g (0.06 mol) of

(7) (a) Makarov, A. Yu.; Kim, S. N.; Gritsan, N. P.; Bagryanskaya, I. Yu.; Gatilov, Yu. V.; Zibarev, A. V. *Mendeleev Commun.* **2005**, 14−17; (b) Shuvaev, K. V.; Bagryansky, V. A.; Gritsan, N. P.; Makarov, A. Yu.; Molin, Yu. N.; Zibarev, A. V. *Mendeleev Commun.* **2003**, 178−179. (c) Vlasyuk, I. V.; Bagryansky, V. A.; Gritsan, N. P.; Molin, Yu. N.; Makarov, A. Yu.; Gatilov, Yu. V.; Shcherbukhin, V. V.; Zibarev, A. V. *Phys. Chem. Chem. Phys.* **2001**, *3*, 409−415. (d) Gritsan, N. P.; Bagryansky, V. A.; Vlasyuk, I. V.; Molin, Yu. N.; Makarov, A. Yu.; Platz, M. S.; Zibarev, A. V. *Russ. Chem. Bull., Int. Ed. Engl.* **2001**, *50*, 2064−2070.

(8) (a) Komin, A. P.; Street, R. W.; Carmack, M. *J. Org. Chem.* **1975**, *40*, 2749−2752. (b) Kane, J.; Schaeffer, R. *Cryst. Struct. Commun.* **1981**, *10*, 1403−1404. (c) Kwan, C. L.; Carmack, M.; Kochi, J. K. *J. Phys. Chem.* **1976**, *80*, 1786−1792.

(9) (a) Batail, P. *Chem. Rev.* **2004**, *104*, 4887−4890 (and other papers of this special issue dedicated to molecular conductors). (b) Gatteschi, D. *Monat. Chem.* **2003**, *134*, 113−115 (and other papers of this special issue dedicated to molecular magnets).

(10) Sheldrick, G. M. *SHELX-97- Programs for Crystal Structure Analysis (release 97.2)*; Göttingen University: Göttingen, Germany.

(11) Sheldrick, G. M. *SADABS-Program for empirical X-ray absorption correction*; Bruker-Nonius: Karlsruhe, Germany, 1990−2004.

(12) Frisch, M. J.; Trucks, G. W.; Schlegel, H. B.; Scuseria, G. E.; Robb, M. A.; Cheeseman, J. R.; Zakrzewski, V. G.; Montgomery, J. A., Jr.; Stratmann, R. E.; Burant, J. C.; Dapprich, S.; Millam, J. M.; Daniels, A. D.; Kudin, K. N.; Strain, M. C.; Farkas, O.; Tomasi, J.; Barone, V.; Cossi, M.; Cammi, R.; Mennucci, B.; Pomelli, C.; Adamo, C.; Clifford, S.; Ochterski, J.; Petersson, G. A.; Ayala, P. Y.; Cui, Q.; Morokuma, K.; Malick, D. K.; Rabuck, A. D.; Raghavachari, K.; Foresman, J. B.; Cioslowski, J.; Ortiz, J. V.; Stefanov, B. B.; Liu, G.; Liashenko, A.; Piskorz, P.; Komaromi, I.; Gomperts, R.; Martin, R. L.; Fox, D. J.; Keith, T.; Al-Laham, M. A.; Peng, C. Y.; Nanayakkara, A.; Gonzalez, C.; Challacombe, M.; Gill, P. M. W.; Johnson, B. G.; Chen, W.; Wong, M. W.; Andres, J. L.; Head-Gordon, M.; Replogle, E. S.; Pople, J. A. *Gaussian 98*, revision A.7; Gaussian, Inc.: Pittsburgh, PA, 1998.

(13) Geisel, M.; Mews, R. *Chem. Ber.* **1982**, *115*, 2135−2140.

freshly calcinated CsF in 100 mL of the same solvent. After an additional 1 h, the reaction mixture was cooled to 20 °C, filtered, and the solvent was distilled off under reduced pressure. The residue was sublimed under vacuum and recrystallized from hexane. Compound **1** was obtained as long, colorless needles, 2.68 g (62%), mp = 117−118 °C. MS, *m*/*z*: 143.9570 (M^+, calculated for $C_2N_4S_2$ 143.9564). NMR ($CDCl_3$), δ ^{13}C: 169.5; ^{15}N: 315.4. UV−vis (EtOH) λ_{max}/nm (log ϵ): 316 (4.35).

Chemical Generation of 2. In an ESR tube, a solution of 0.0288 g (0.2 mmol) of **1** and 0.0448 g (0.4 mmol) of *t*-BuOK in 1 mL of absolute MeCN, degassed by three freeze−pump−thaw cycles, was heated to 50 °C for 20 min. After the mixture was cooled to 25 °C, the ESR spectrum of the reaction solution was recorded to be identical to that of electrochemically prepared **2**.

Preparation of 8 and 9. A solution of 0.103 g (0.2 mmol) of salt **7** in 0.5 mL of absolute MeCN was kept for 3 days at 20 °C (in the case of **8**) or at −20 °C (in the case of **9**). The crystals formed were filtered off and identified by XRD as salts **8** or **9**. Salt **8**: 0.012 g, dark-red plates, mp (sealed capillary) = 135 °C (dec). Salt **9**: 0.013 g, red prisms, mp (sealed capillary) = 125 °C (dec).

Synthesis of 4 and 5. (a) At 20 °C, to a stirred solution of 8.24 g (0.04 mol) of $(Me_3SiN{=})_2S$[14b] in 20 mL of CH_2Cl_2 was added dropwise a solution of 5.74 g (0.04 mol) of C_6H_5SCl in 15 mL of CCl_4. After 16 h, the solvent was distilled off and the residue distilled under vacuum. Compound **4** was obtained as red oil, 7.42 g (77%), bp = 78−79 °C/0.01 Torr. Low-temperature crystallization from hexane gave **4** as orange prisms, mp = 22−23 °C. MS, *m*/*z*: 242.0365 (M^+, calculated for $C_9H_{14}N_2S_2Si$ 242.0368). NMR ($CDCl_3$), δ ^{1}H: 7.59, 7.38, 7.23, 0.39; ^{13}C: 137.0, 128.5, 126.4, 124.5, 1.4; ^{15}N: 303.2, 296.6; ^{29}Si: 2.7. UV−vis (heptane) λ_{max}/nm (log ϵ): 385 (4.31). Found (Calcd for $C_9H_{14}N_2S_2Si$), %: C, 44.6 (44.59); H, 5.75 (5.82); N, 11.6 (11.56); S, 26.3 (26.45). (b) At −30 °C, to a stirred solution of 9.07 g (0.044 mol) of $(Me_3SiN{=})_2S$[14b] in 50 mL of hexane was added dropwise a solution of 7.46 g (0.044 mol) of C_6H_5SeCl in 20 mL of hexane and 25 mL of Et_2O. The reaction mixture was warmed slowly to 20 °C, and the solvents were distilled off. The residue was distilled under vacuum. Compound **5** was obtained as orange oil that solidified upon standing, bp = 106−108 °C/0.01 Torr. Crystallization from hexane gave **5** as elongated orange prisms, 6.92 g (61%), mp = 33−35 °C. MS, *m*/*z*: 289.9811 (M^+, Calcd for $C_9H_{14}N_2SSeSi$ 289.9811). NMR ($CDCl_3$), δ ^{1}H: 7.73, 7.41, 7.31, 0.42; ^{13}C: 133.2, 129.1, 128.7, 127.1, 1.3; ^{15}N: 318.2, 302.9; ^{29}Si: 2.8; ^{77}Se: 1156. UV−vis (heptane) λ_{max}/nm (log ϵ): 386 (4.08). Found (Calcd for $C_9H_{14}N_2SSeSi$), %: C, 37.4 (37.36); H, 4.72 (4.88); N, 9.62 (9.68).

Synthesis of 6 and 7. At −40 °C, a solution of 2 mmol of **4** or **5** in 10 mL of THF was added to a solution of 0.75 g (2 mmol) of $[K(18\text{-crown-}6)]^+[t\text{-BuO}]^-$ in 20 mL of the same solvent (prepared from 0.22 g (2 mmol) of *t*-BuOK and 0.53 g (2 mmol) of (18-crown-6) at −20 °C).[15c] After 1 h, the solvent was removed at the same temperature and 15 mL of MeCN was condensed onto the solid residue at −196 °C. On warming to −40 °C, the solution formed was filtered through a sintered glass frit, cooled to −196 °C, and 20 mL of Et_2O were condensed onto it. The reaction system was placed into a cryostat at −30 °C for crystal growth. Salts **6** and **7** were obtained as yellow crystalline solids after removing the solvents with a syringe and drying the residue in a vacuum. Salt **6**: 0.47 g (50%), mp = 129 °C (dec). NMR (CD_3CN), δ ^{1}H: 7.33, 7.21, 6.94, 3.55; ^{13}C: 144.8, 129.2, 124.3, 123.7, 70.8. Found (Calcd for $C_{18}H_{29}KN_2O_6S_2$), %: C, 45.6 (45.74); H, 6.17 (6.18); S, 13.6 (13.57). Salt **7**: 0.89 g (87%), mp = 130 °C (dec). NMR (CD_3CN), δ ^{1}H: 7.73, 7.28, 6.98, 3.53; ^{77}Se: 763. Found (Calcd for $C_{18}H_{29}KN_2O_6SSe$), %: C, 41.8 (41.61); H, 5.59 (5.63); N, 5.30 (5.39).

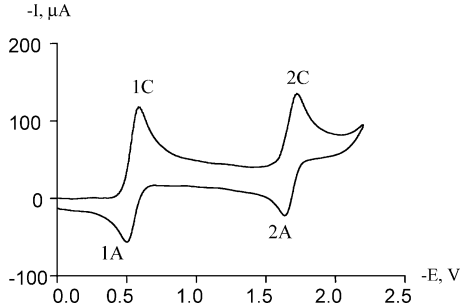

Figure 1. CV of **1** (2 10^{-3}M, scan rate 100 mV s^{-1}).

Scheme 1

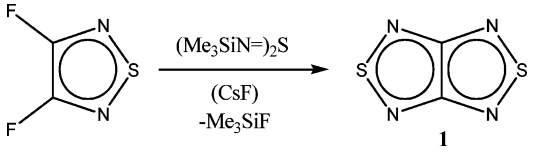

Scheme 2

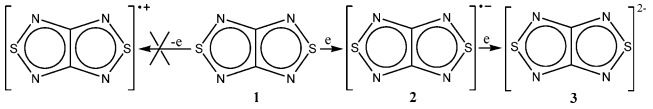

Results and Discussion

Compound **1** was prepared by an extension of the arylthiazylamide-based[15] methodology (previously suggested for the synthesis of 2,1,3-benzothiadiazoles)[14] to nonbenzoid systems (Scheme 1).

Cyclic voltammetry (CV) on a solution of **1** in MeCN in the potential range from −2.5 to 2.5 V revealed no oxidation waves but two reversible one-electron reduction waves (Figure 1) at −0.59 (1C) and −1.72 V (2C) corresponding to consecutive transformations of **1** into the radical anion **2** and the dianion (**3**) (Scheme 2). Oxidation peaks 1A and 2A (Figure 1) observed even at low scan rates (∼20 mV s^{-1}) evidence that **2** and **3** are rather long-lived species. The relation of anodic and cathodic currents, $I_p^A/I_p^C < 1$ for both 1C and 2C peaks, indicates that **2** and **3** are involved into further chemical transformations. The disproportionation 2 **2** → **1** + **3** seems unlikely since its equilibrium constant can be estimated from the CV data as $K \approx 10^{-19}$ (Figure 1).

The formation of **2** is confirmed by ESR spectroscopy (Figure 2). For **2**, the hfc constant $a(^{14}N \times 4) = 0.314$ mT (previously reported, 0.317 mT;[8c] calculated by DFT/

(14) (a) Zibarev, A. V.; Miller, A. O. *J. Fluorine Chem.* **1990**, *50*, 359−363. (b) Bagryanskaya, I. Yu.; Gatilov, Yu. V.; Miller, A. O.; Shakirov, M. M.; Zibarev, A. V. *Heteroatom Chem.* **1994**, *5*, 561−565. (c) Lork, E.; Mews, R.; Shakirov, M. M.; Watson, P. G.; Zibarev, A. V. *Eur. J. Inorg. Chem.* **2001**, 2123−2134. (d) Makarov, A. Yu.; Bagryanskaya, I. Yu.; Blockhuys, F.; Van Alsenoy, C.; Gatilov, Yu. V.; Knyazev, V. V.; Maksimov, A. M.; Mikhalina, T. V.; Platonov, V. E.; Shakirov, M. M.; Zibarev, A. V. *Eur. J. Inorg. Chem.* **2003**, 77−88.

(15) (a) Zibarev, A. V.; Lork, E.; Mews, R. *Chem. Commun.* **1998**, 991−992. (b) Borrmann, T.; Lork, E.; Mews, R.; Stohrer, W.-D.; Watson, P. G.; Zibarev, A. V. *Chem. Eur. J.* **2001**, *7*, 3504−3510. (c) Borrmann, T.; Lork, E.; Mews, R.; Shakirov, M. M.; Zibarev, A. V. *Eur. J. Inorg. Chem.* **2004**, 2452−2458.

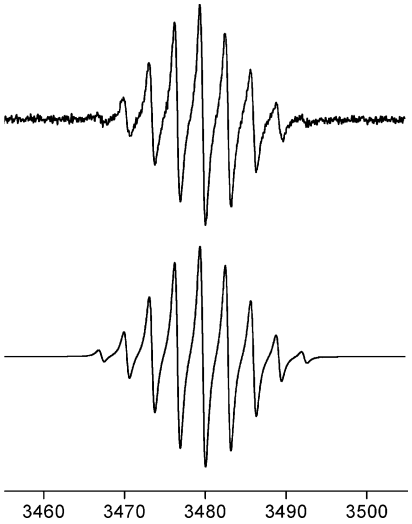

Figure 2. Experimental (above) and simulated (below) ESR spectrum of **2** from electrochemical reduction of **1** ($|H|$ 10^4 T^{-1}).

Table 2. Selected Bond Lengths, Bond Angles, and Torsion Angles for **6** and **7**

bond (pm)/angle (°)	**6** (X = S)	**7** (X = Se)
C−X	176.3(7)	190.6(8)
X−N	169.8(6)	185.8(7)
N═S	159.1(6)	157.9(8)
S═N	147.8(6)	148.3(8)
C−X−N	100.7(3)	97.0(4)
X−N═S	114.7(3)	113.1(4)
N═S═N	122.2(3)	121.2(4)
C−C−X−N	3.6(6)	6.4(8)
C−X−N═S	−175.9(4)	−165.4(5)

Table 3. Molecular Geometries of **1**−**3**

	1		**2**			**3**
			XRD		UB3LYP	B3LYP
bond (pm)/angle (°)	XRD[a]	B3LYP	salt **8**	salt **9**		
N1−S2	161.9(2)	163.8	165.2(2)	165.9(2)	169.2	171.7
S2−N3	161.9(2)	163.8	165.7(2)	165.4(2)	169.2	171.7
N3−C3a	135.1(3)	133.9	135.2(3)	134.2(3)	133.6	131.0
C3a−N4	134.8(3)	133.9	131.7(3)	134.2(3)	133.6	131.0
N4−S5	161.9(2)	163.8	165.2(2)	165.4(2)	169.2	171.0
S5−N6	161.9(2)	163.8	165.7(2)	165.9(2)	169.2	171.0
N6−C6a	135.1(3)	133.9	135.2(3)	133.3(2)	133.6	131.0
C6a−N1	134.8(3)	133.9	131.7(3)	133.3(2)	133.6	131.0
C3a−C6a	142.9(4)	146.3	146.6(4)	145.0(4)	148.7	151.4
C6a−N1−S2	104.3(2)	104.7	105.2(2)	104.7(2)	105.0	106.5
N1−S2−N3	103.0(1)	102.5	101.3(1)	101.5(1)	100.6	98.2
S2−N3−C3a	104.4(2)	104.7	105.2(2)	104.5(2)	105.0	106.5
C3a−N4−S5	104.3(2)	104.7	105.5(2)	104.5(2)	105.0	106.5
N4−S5−N6	103.0(1)	102.5	101.3(1)	101.5(1)	100.6	98.2
S5−N6−C6a	104.4(2)	104.7	105.2(2)	104.7(2)	105.0	106.5
N1−C6a−C3a	114.4(2)	114.0	115.5(3)	114.6(1)	114.7	114.4
C6a−C3a−N3	113.9(2)	114.0	112.8(3)	114.7(2)	114.7	114.4
N4−C3a−C6a	114.9(2)	114.0	115.5(3)	114.7(2)	114.7	114.4
N6−C6a−C3a	113.9(2)	114.0	112.8(3)	114.6(1)	114.7	114.4

[a] Due to relatively low accuracy of published room-temperature data,[8b] the structure of **1** was redetermined.

UB3LYP/6-311+G*, 0.238 mT) and $g = 2.0045$. On the basis of the ESR data, a half-life time of the electrochemically generated **2** can be estimated as $\tau_{1/2} = 74.5$ s.

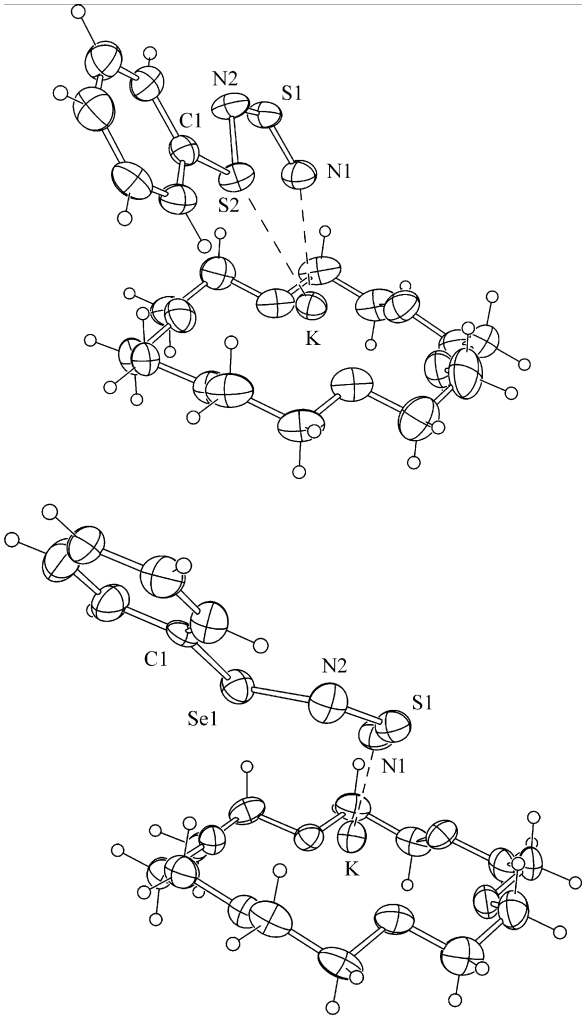

Figure 3. Structure of salts **6** (above) and **7** (below) (for bond lengths and bond angles, see Table 3). Dashed lines indicate shortened contacts (pm). Salt **6**: $K^+\cdots$N1, 276.9(6); $K^+\cdots$S2, 370.0(2). Salt **7**: $K^+\cdots$N1, 268.9(8).

The redox behavior of **1** is different from that of its 10π-electron carbon analogue, naphthalene, which can be oxidized irreversibly at $E_p^{ox} = 1.73$ V ($E_{1/2}^{ox} = 1.54$ V),[1b] and reduced reversibly at $E_p^{red} = -2.63$ V ($E_{1/2}^{red} = -2.50$ V).[1b] The redox properties of numerous S−N ring systems related to **1** have recently been reviewed.[1b]

Salts [K(18-crown-6)][**2**] and [K(18-crown-6)][**2**]·MeCN, (**8**) and (**9**) respectively, were obtained in low yield as products of spontaneous transformations of [K(18-crown-6)][PhXNSN] salts (**6**, **7**; X = S, Se) in MeCN solution. Salts **6** and **7** were prepared by desilylation of the precursors Ph−S−N═S═N−$SiMe_3$ (**4**) and Ph−Se−N═S═N−$SiMe_3$ (**5**) with $[K(18\text{-crown-6})]^+[t\text{-BuO}]^-$ (Scheme 3), and their structures were confirmed by XRD (Figure 3, Tables 1 and 2; cf. $[K(18\text{-crown-6})]^+[PhNSN]^-$).[15c] (A detailed discussion

Scheme 3

$$(Me_3SiN=)_2S \xrightarrow[-Me_3SiCl]{PhXCl} \underset{\mathbf{4},\ \mathbf{5}}{Ph\text{-}X\text{-}N=S=N\text{-}SiMe_3} \xrightarrow[-Me_3Si\text{-}O\text{-}Bu\text{-}t]{[K(18\text{-crown-6})]^+[t\text{-BuO}]^-} \underset{\mathbf{6},\ \mathbf{7}}{[K(18\text{-crown-6})]^+[PhXNSN]^-}$$

X = S (**4**, **6**), Se (**5**, **7**)

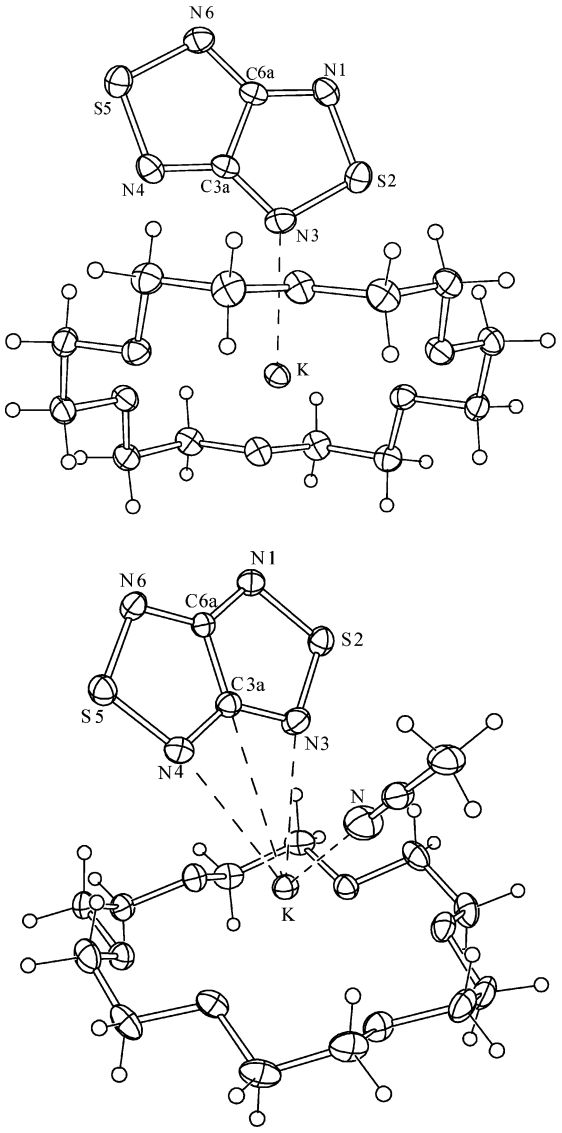

Figure 4. Structure of salts **8** (above) and **9** (below) (for bond lengths and bond angles, see Table 3). Dashed lines indicate shortened contacts (pm). Salt **8**: $K^+\cdots$N3, 288.5(2). Salt **9**: $K^+\cdots$N3, 298.3(2) Å; $K^+\cdots$N4, 298.3(2) Å; $K^+\cdots NCCH_3$, 2.842(3).

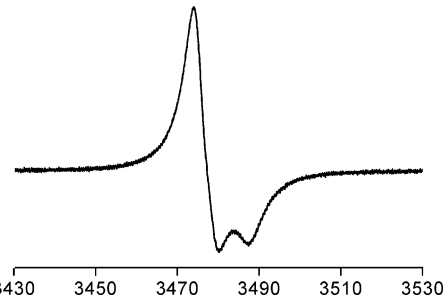

Figure 5. Anisotropic ESR spectrum of crystalline salt **8** ($|H|$ 10^4 T^{-1}).

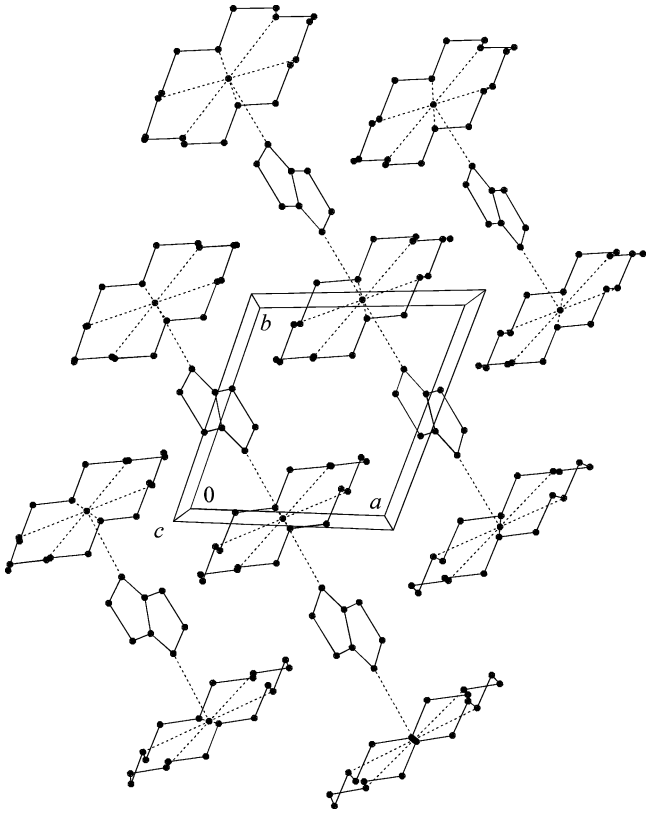

Figure 6. Crystal packing of salt **8** viewed along the *c* axis.

of the structures of salts **6** and **7** will be presented in a special paper on various $PhXNSN^-$ salts).[16]

The structures of the radical anion salts **8** and **9** are confirmed by XRD (Tables 1 and 3, Figure 4). The ESR spectra of crystalline **8** and **9** are not resolved (Figure 5), but those of their solutions in MeCN are identical to the spectrum of the electrochemically generated **2** (Figure 2). Salts **8** and **9** are thermally stable but very moisture sensitive.

The crystal packing of salts **8** and **9** is different. In particular, the radical anion **2** acts as a bridging ligand in **8** (Figure 6) and as chelating ligand in **9** (Figure 7). The long distances between radical anions **2** exclude their interaction in the crystal, and one can expect **8** and **9** to be paramagnetic (Mott) insulators.[9a] With cations significantly smaller than $[K(18\text{-crown-}6)]^+$, however, it seems possible to obtain packing patterns favorable to effective interactions between the particles **2**.

Recently, DFT calculations with the B3LYP hybrid functional have been shown to be a reliable approach to molecular geometries, isotropic hfc constants, and redox characteristics of various heterocyclic thiazyl radicals.[5] Figure 8 depicts the HOMO of **1** ($-\epsilon_i = 8.06$ eV) and the SOMO of **2** ($-\epsilon_i = 0.35$ eV) from DFT/(U)B3LYP/6-311+G* calculations. These data explain the failure of the electrochemical approach to the radical cation of **1** (the HOMO is highly stabilized by four electronegative N atoms), as well as the structural changes in going from **1** to **2**, especially the elongation of the S−N bonds and insensitivity of the C−N bonds (the SOMO is antibonding for S−N and nonbonding for C−N bonds). The elongation of the C−C bond in **2** (XRD) seemingly compensates for ring strain induced by the elongated S−N bonds and the almost unaffected N−S−N angles (Table 3). In going from **2** to **3**, the SOMO of the former transforms into the HOMO of the

(16) Makarov, A. Yu.; Lork, E.; Mews, R.; Zibarev, A. V. paper in preparation.

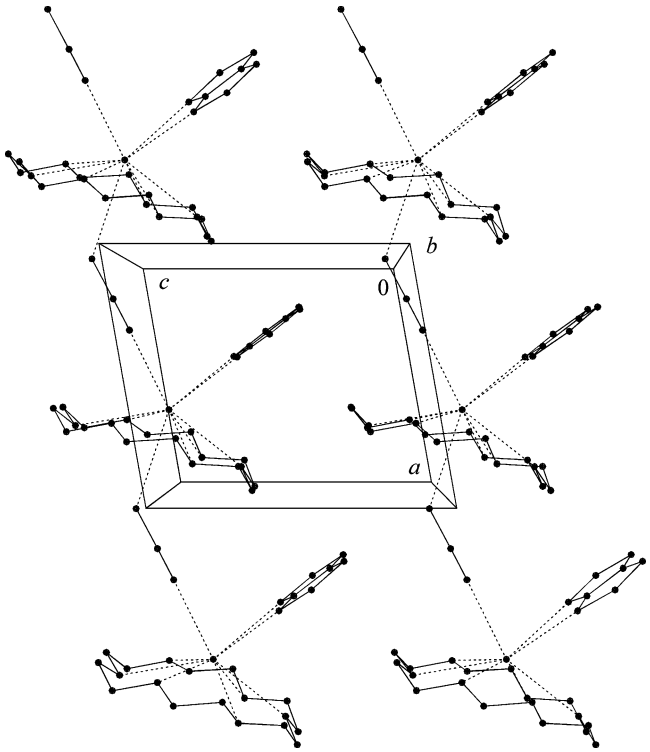

Figure 7. Crystal packing of salt **9** viewed along the *b* axis.

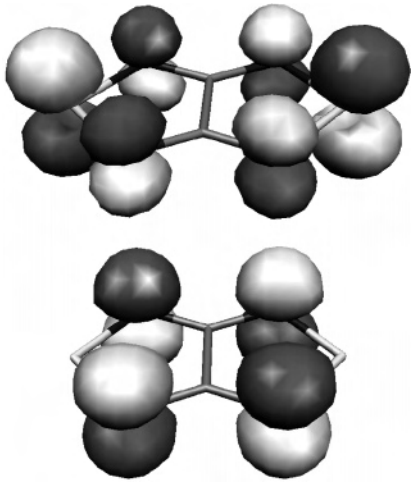

Figure 8. The SOMO of **2** (above) and the HOMO of **1** (below).

latter and the corresponding elongation of the S−N bonds of **3** reflects the essentially antibonding character of this MO.

The origin of radical anion **2** in the discussed transformations of salts **6** and **7** leading to salts **8** and **9**, which evidently requires the participation of MeCN as a source of carbon, is not entirely clear. Under the same conditions (20 °C, MeCN), decomposition of salt **7** proceeds faster (a few tens of minutes) than that of salt **6** (a few days). In the case of precursor **7**, the ^{77}Se NMR spectra of the reaction solutions after precipitation of crystalline salts **8** or **9** contained a single peak in the δ ^{77}Se range of 384−355 ppm (depending on the sample), which can be assigned to a mixture of $PhSe^-$ and PhSeSePh.[17] In both cases, the ^{14}N NMR spectra of these

Scheme 4

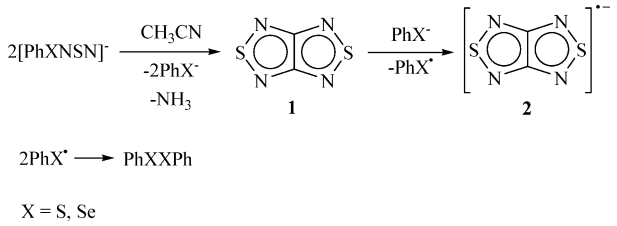

solutions revealed signal at −8 ppm which can be assigned to dissolved NH_3.[18] On the basis of these observations, one might tentatively suggest Scheme 4 for the discussed decomposition of salts **6** and **7** in MeCN solution. The reaction involves cleavage of the X−N bond of the $[PhXNSN]^-$ anions (X = S, Se) with formation of PhX^- anions. The latter reduces released **1** into **2**, the byproducts are PhXXPh (X = S, Se) and arise from recombination of the corresponding $PhX^\bullet$ radicals (Scheme 4). Since the precursors **6** and **7** are soluble only in MeCN, no other solvents have been tried.

Besides electrochemical reduction, **1** can also be reduced chemically into **2**, for example, by the action of *t*-BuOK in MeCN. The ESR spectrum of the reaction mixture is identical to that observed for electrochemically generated **2** (Figure 2) and solutions of salts **8** and **9**.

Conclusions

The reversible electrochemical reduction of the precursor [1,2,5]thiadiazolo[3,4-c][1,2,5]thiadiazole (**1**) to the long-lived title radical anion **2**,[8c] a rare example of heterocyclic thiazyl radical anions, was confirmed by ESR spectroscopy. Further reduction reversibly leads to the dianion **3**. Radical anion **2** is also obtained by the chemical reduction of the precursor **1**. Unexpectedly, the radical anion **2** is also formed in the decomposition of [K(18-crown-6)][PhXNSN] salts (**6**, **7**; X = S, Se) in MeCN solution to give thermally stable salts with the $[K(18\text{-crown-6})]^+$ cation (**8**, **9**). This behavior of **6** and **7** is very different from that of related salts of $[RNSN]^-$ (R = Ar, Alk), anions which are stable in MeCN solutions.[15c] Experiments based on the aforementioned findings and designed to prepare bulky samples of stable salts of **2** with various cations via chemical reduction from **1** with different reduction agents are in progress. Electrical and magnetic measurements on these samples are also planned because salts with **2** might be of interest to materials science as building blocks for molecular ion-based conductors and/or magnets.

Further development in this field might also be associated with the Se analogue of **1**, [1,2,5]selenadiazolo[3,4-c][1,2,5]-thiadiazole,[19] and its still unknown bis-selenium derivative.

IC050583J

(17) Jacobson, B. M.; Kook, A. M.; Lewis, E. S. *J. Phys. Org. Chem.* **1989**, *2*, 410−416.
(18) Mason, J. *Chem. Rev.* **1981**, *81*, 205−221.
(19) Komin, A. P.; Carmack, M. *J. Heterocyclic Chem.* **1976**, *13*, 13−22.